Pharm Res (2015) 32:389–402
DOI 10.1007/s11095-014-1469-1

RESEARCH PAPER

Enhanced Oral Delivery of Curcumin from N-trimethyl Chitosan Surface-Modified Solid Lipid Nanoparticles: Pharmacokinetic and Brain Distribution Evaluations

Prakash Ramalingam • Young Tag Ko

Received: 8 May 2014 / Accepted: 24 July 2014 / Published online: 1 August 2014

ABSTRACT

Purpose Solid lipid nanoparticles (SLNs) have been proposed as a colloidal carrier system that could enhance the oral bioavailability of curcumin. However, a burst release of the loaded drug, which occurs in acidic environments, has been a main obstacle to the oral delivery of curcumin by using SLNs as a carrier system. We hypothesized that a quarternized chitosan derivative could be used for acid-resistant coating to stabilize the SLNs and circumvent the burst release.

Methods *N*-trimethyl chitosan (TMC) was synthesized and determined by ^{1}H-NMR and FT-IR. To investigate the details of chitosan and TMC surface modification on SLCNs composed of palmitic acid, cholesterol, TPGS and curcumin, a number of factors such as optimized SLNs composition, solid state characterization, stability, cell viability, *in vitro* release in GI conditions, curcumin oral bioavailability and brain distribution studies, were evaluated.

Results The TMC-SLCNs exhibited prolonged stability in room and refrigerated conditions, controlled drug release in simulated intestinal fluid, significantly higher oral bioavailability, and brain distribution of curcumin than free curcumin, chitosan and non-coated SLCNs.

Conclusions These finding suggests that the TMC-SLCNs is a promising nanocarrier system for oral delivery and brain distribution of curcumin.

KEY WORDS coating · curcumin · *N*-trimethyl chitosan · oral drug delivery · solid lipid nanoparticles

ABBREVIATIONS

CH-SLCNs	Chitosan coated solid lipid nanoparticles
DSC	Differential scanning calorimetry
FT-IR	Fourier transform-infrared spectroscopy
H-NMR	Proton nuclear magnetic resonance spectroscopy
HPLC	High performance liquid chromatography
LC-MS/MS	Liquid chromatography – tandem mass spectroscopy
MTT reagent	(3-[4, 5-dimethyl –thiazol-2-yl]-2, 5-diphenyl tetrazolium bromide)
PXRD	Powder X-ray diffraction
SLCNs	Curcumin-loaded solid lipid nanoparticles
SLNs	Solid lipid nanoparticles
TGA	Thermogravimetric analysis
TMC	*N*-trimethyl chitosan
TMC-SLCNs	*N*-trimethyl chitosan coated solid lipid nanoparticles
TPGS	D-α-tocopheryl polyethylene glycol 1,000 succinate

P. Ramalingam · Y. T. Ko (✉)
College of Pharmacy, Gachon University
191 Hambakmoero, Yeonsu-gu, Incheon
406-799, South Korea
e-mail: youngtakko@gachon.ac.kr

INTRODUCTION

Curcumin, a lipophilic polyphenolic compound extracted from *Curcuma longa*, exhibits a broad range of biological and pharmacological activities, including anti-amyloid, anti-oxidant, anti-malarial, anti-inflammatory, anti-HIV, and anti-tumor properties (1,2). Curcumin is a well-known multitherapeutic and chemotherapeutic agent with demonstrated effectiveness against various types of cancer, including tumors of the lung, breast, head-neck, bone, prostate, and gastrointestinal tract (3). Despite its valuable therapeutic effects, clinical use of curcumin is restricted by pharmacokinetic obstacles such as poor oral bioavailability due to low water solubility, instability at neutral and alkaline pH values, extensive metabolism, and rapid elimination (4).

Over the last few decades, considerable attention has been focused on designing novel drug delivery carrier systems that would enhance the oral bioavailability of lipophilic drugs.

SLNs are among the most popular drug delivery systems and have been reported to have potential for sustained delivery of orally administered lipophilic drugs. In addition to their non-toxic nature and high payload capacity, SLNs, as a nanocarrier system, have the ability to augment the solubility, bioavailability, and stability of the drug they carry (5,6). However, variable release patterns of drug-loaded SLNs in the gastrointestinal tract have been a major obstacle to their wide application for oral delivery of lipophilic drugs. Drug-loaded SLNs exhibit a burst release of drugs in the acidic environment of the stomach lumen (pH 1–3) and a sustained release in the intestinal environment (pH 6.8–7.4) (7–9). Considering all these concerns, as well as the positive aspects of SLN formulations, we designed surface-modified SLNs that minimize the burst release of the carried drug in the gastric milieu.

Chitosan, a cationic natural polysaccharide derived from deacetylated chitin, exhibits excellent properties for biological applications, including high biocompatibility, biodegradability, mucoadhesivity, low toxicity, and antimicrobial activity (10). It is soluble at acidic pH conditions, and its protonated form is only active as an absorption enhancer in acidic environments. Chitosan is a weak base and a sufficient amount of acid is required for conversion of the glucosamine units into the water soluble positively charged form. Usage of chitosan for potential oral drug delivery applications is limited by its low solubility in neutral and alkaline environments (11) and the tendency of chitosan molecules to aggregate and lose their positive charge in solutions at physiological pH. Recently, a broad range of chitosan based biomaterials have been developed and utilized in novel drug delivery systems based on chemical modifications of chitosan (12). Methylation of chitosan introducing trimethyl group moieties into the polymer backbone significantly improved the aqueous solubility (13). TMC, a quaternized chitosan derivative, shows excellent aqueous solubility over a wide pH range, in addition to mucoadhesive and absorption-enhancing properties at neutral pH (14). Among the plethora of polymeric materials, TMC, a water soluble cationic polyelectrolyte is useful for the delivery of therapeutic drugs via various route including intravenous, peroral (15), intranasal (14), buccal (16), ocular (17), pulmonary (18) and rectal routes (19). Earlier, many therapeutic moieties including antioxidants, enzymes, vaccines, antimicrobials, and small molecules has been successfully encapsulated and administered *in vivo*. It has also been reported that TMC can decrease the transepithelial electrical resistance (TEER) of CaCo2 cell monolayers and enhance the oral delivery of vaccine (20), insulin (21), cispaltin (22), DNA (23), curcumin (24) and peptides/proteins (12,25). We hypothesized that TMC could provide an acid-resistant alternative to unmodified chitosan for the formation of stable SLNs that will not exhibit burst release.

The lipid matrix derived from physiological lipid components reduces the danger of acute and chronic toxicity (5). Palmitic acid, cholesterol and TPGS [GRAS (generally regarded as safe) grade], and their application for the delivery of active ingredient is approved by regulatory authorities. The addition of TPGS as an emulsifier and stabilizer to lipid based formulations may enhance the solubility, oral bioavailability and stability of entrapped compounds (26). In this study, SLCNs were formulated using palmitic acid (CH_3 $(CH_2)_{14}$ COOH), cholesterol, TPGS, and curcumin, and their ability to enhance the solubility, stability and oral bioavailability of curcumin was tested using *in vitro* and *in vivo* assays. The comparative physicochemical characteristics, physical stability, release, and pharmacokinetics of non-modified SLCNs, CH-SLCNs and TMC-SLCNs were studied for the designing a novel drug carrier system suitable for oral administration of curcumin (Fig. 1). In order to enhance the potential application of curcumin against Alzheimer's disease and brain gliomas, we further analyzed curcumin concentration in the whole brain, capillary fraction (the pellet) and a supernatant fraction of brain parenchyma.

MATERIALS AND METHODS

Materials

Chitosan (molecular weight, 15 kDa) was purchased from Polysciences, Inc. (Warrington, PA, USA). Curcumin, resveratrol internal standard, and *N*-methyl-2-pyrollidinone (NMP) were purchased from the TCI Co., Ltd (Tokyo, Japan). Salbutamol, methyl iodide, sodium iodide, sodium hydroxide, sodium chloride, palmitic acid and, TPGS were purchased from Sigma- Aldrich Co. (St. Louis, MO, USA). Cholesterol was purchased from Wako Pure Chemical Industries, Ltd. (Osaka, Japan). The solvents acetonitrile (Avantor, PA, USA) and water (Fisher Scientific Korea Ltd, Korea) were of HPLC grade. All other chemicals and reagents used in this study were of analytical grade and used without further purification.

Preparation and Characterization of TMC

TMC polymer was synthesized and characterized according to the previously established procedure (14), with the two-step methylation pathway depicted in Fig. 2a. Briefly, 1 g of chitosan and 2.4 g of sodium iodide were dissolved in a mixture of 40 mL of NMP and 6 mL of 15% aqueous sodium hydroxide solution in a heated water bath at 60°C with stirring. Once chitosan was dissolved, 6.5 mL of methyl iodide was added to the reaction mixture and stirred for 1 h. The product was precipitated using 200 mL of an ethanol/diethyl ether mixture. Isolated by centrifugation, and washed with diethyl ether. The product was dissolved in 20 mL of deionized water and 125 ml of 1 M HCl was added to change the counterion from iodide to chloride. Synthesis of TMC with a

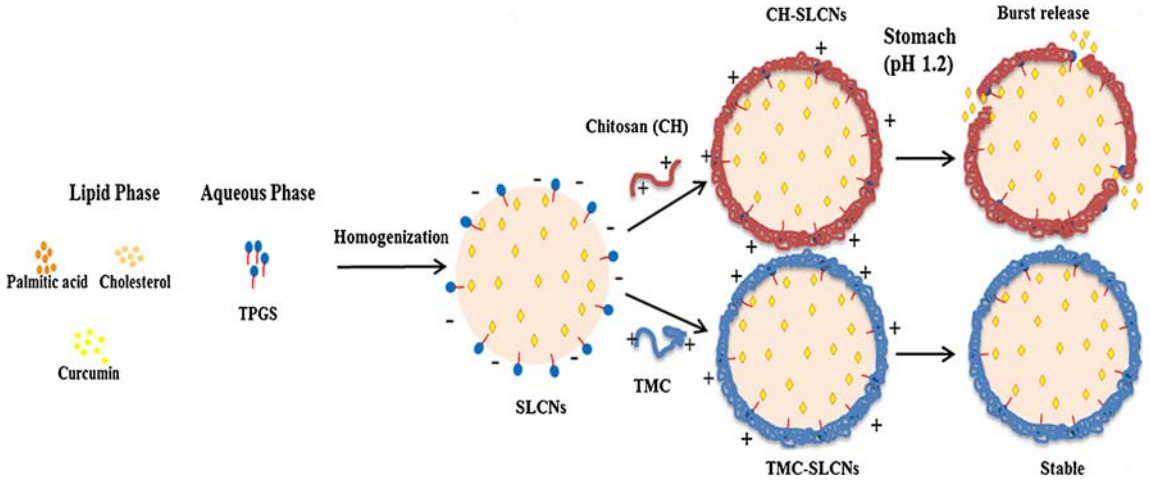

Fig. 1 Schematic illustration of surface modification on SLCNs with chitosan and TMC for curcumin oral delivery.

high degree of quaternization required additional steps: before precipitation, 3 mL of methyl iodide and 3 mL of 15% sodium hydroxide were added to and the mixture stirred for another 1 h. For the highly quaternized TMC, the final reaction product was dissolved in 20 mL of 10% NaCl (instead of HCl) to exchange the iodide. The resulting product was precipitated by centrifugation after ethanol addition and washed with diethyl ether. After drying at 40°C under vacuum, TMC was obtained as a white, and water- soluble solid.

The ^{1}H-NMR spectrum of the purified TMC was acquired with a Bruker 600 MHz Nuclear Magnetic Resonance Spectrometer (Bruker Analytik, Germany). A 2 mg sample of the polymer product was dissolved in 700 µL of D_2O for analysis. The extent of *N*-trimethyl group incorporations, considered an index of the degree of quaternization (DQ) was determined by ^{1}H-NMR using the following equation:

$$\mathrm{DQ} = \left[\frac{[CH3]3}{[H]} \times \frac{1}{9}\right] \times 100$$

where, $[CH_3]_3$ is the integral of the peaks corresponding to the nine hydrogen atoms from the trimethylated amino groups at 3.3 ppm, and [H] is the integral of ^{1}H peaks between 4.7 and 5.7 ppm (reference signals), representing the hydrogen atom bound to the C-1 of the glycopyranose ring of the glucosamine (20).

FT-IR spectra of chitosan and TMC were recorded using four scans obtained using a spectrophotometer (Bruker

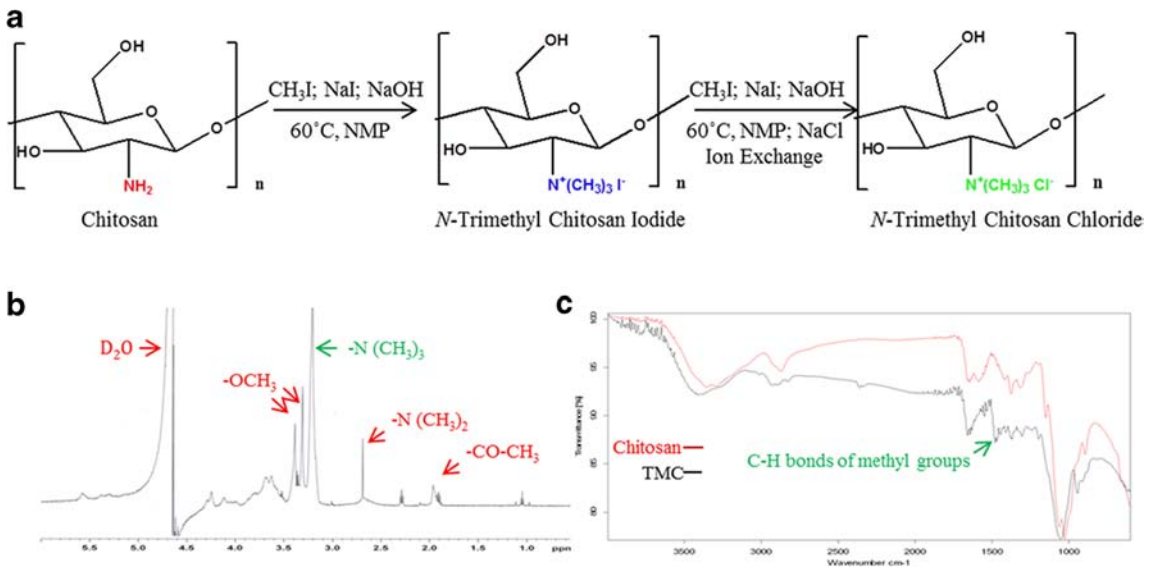

Fig. 2 Scheme for the synthesis of TMC (**a**); ^{1}H-NMR (**b**) and FT-IR spectra (**c**).

Analytik, Rheinstetten, Germany) operating in the region from 4,000 to 500 cm^{-1} with a resolution of 2 cm^{-1}.

Preparation and Characterization of SLCNs

Optimization of SLCNs Composition

SLCNs were prepared by high-shear homogenization and ultra-sonication technique (27), with the compositions of SLCN formulations evaluated and presented in Table I. Briefly, the lipid phase palmitic acid and cholesterol were heated to 5–10°C above their melting point to completely melt the lipid. Curcumin was dispersed into the melted lipid phase. The preheated aqueous solution containing TPGS was added to the lipid phase and homogenization was performed using Ultra-Turrax homogenizer (IKA-Werke, Staufen Germany) for 5 min at 11,000 rpm. The resulting pre-emulsion was sonicated using a probe sonicator (Vibracell VCX130; Sonics, USA) for 5 min. The resulting SLCNs were lyophilized by using freeze-drying (Scan Vac, South Korea) and stored at 4°C for further experiments.

Particle Size, Polydispersity Index (PDI) and Zeta Potential Analysis

The SLCNs were dispersed in distilled water at appropriate concentrations. The mean particle size, poly dispersity index (PI), and zeta potential were measured using the zeta potential and particle size analyzer ELSZ-1000 (Photal OTSUKA Electronics, Tokyo, Japan) based on the dynamic light scattering method. All measurements were performed in triplicate.

Determination of Encapsulation Efficiency and Loading Capacity

Following SLCN synthesis, the quantity of unencapsulated curcumin was measured by ultracentrifugation with Amicon® filter tubes (Millipore, Carrigtwohill, Ireland). Briefly, 500 μL of SLCNs was transferred into a 0.5 mL of centrifugal filter tube and centrifuged at 14,000 rpm for 30 min at 4°C. The amount of unencapsulated curcumin in the supernatant was determined by HPLC with UV detection. The encapsulation efficiency (EE) and loading capacity (LC) were calculated using the following equations:

$$\text{Encapsulation efficiency(EE)} = \frac{T_{Cur} - S_{Cur}}{T_{Cur}} \times 100$$

$$\text{Loading capacity (LC)} = \frac{T_{Cur} - S_{Cur}}{T_L} \times 100$$

where T_{Cur} is the total amount of curcumin in the SLCNs, S_{Cur} is the amount of curcumin measured in the supernatant, and T_L is the total mass of lipids in the SLCNs.

HPLC Analysis

The analytical technique used to quantify curcumin was based on the method described with (28) minor modifications. Briefly, An Agilent 1100 series HPLC system with a variable wavelength detector was used for quantification of curcumin. Sepax BR-C18 column (5 μm, 120 Å 4.6×150 mm) was used with acetonitrile and water (1:1) (v/v) as the mobile phase. Curcumin from different SLN formulations was analyzed following the addition of resveratrol as an internal standard, liquid-liquid extraction with ethyl acetate and dilution in the appropriate volume of the mobile phase. A 20 μL aliquot was

Table I Development and Optimization of SLCNs (mean ± S.D, $n = 3$)

Formulation code	Composition[a]	Particle size		Zeta potential (mV)	EE (%)	LC (%)
		Mean size (nm)	PDI			
P1	20 : 3 : 8 : 1	243.6 ± 15.8	0.17 ± 0.04	−28.57 ± 1.31	93.23 ± 0.06	4.05 ± 0.01
P2	30 : 3 : 8 : 1	388.1 ± 24.9	0.24 ± 0.02	−29.15 ± 2.05	92.96 ± 0.11	4.04 ± 0.01
P3	40 : 3 : 8 : 1	513.9 ± 71.3	0.29 ± 0.01	−30.37 ± 1.29	92.83 ± 0.05	4.03 ± 0.01
C1	20 : 6 : 8 : 1	294.0 ± 21.7	0.25 ± 0.02	−29.62 ± 0.80	93.20 ± 0.10	4.05 ± 0.01
C2	20 : 4 : 8 : 1	219.8 ± 10.4	0.16 ± 0.01	−28.83 ± 1.83	93.16 ± 0.05	4.05 ± 0.01
C3	20 : 2 : 8 : 1	190.7 ± 15.1	0.19 ± 0.01	−28.34 ± 1.11	93.10 ± 0.10	4.04 ± 0.01
T1	20 : 2 : 12 : 1	223.9 ± 14.3	0.21 ± 0.09	−26.80 ± 1.76	92.70 ± 0.06	4.03 ± 0.01
T2	20 : 2 : 10 : 1	179.1 ± 11.5	0.20 ± 0.03	−26.60 ± 0.57	93.07 ± 0.06	4.04 ± 0.01
T3	20 : 2 : 6 : 1	138.8 ± 7.6	0.15 ± 0.04	−29.67 ± 1.20	93.13 ± 0.11	4.05 ± 0.01
T3-1	20 : 2 : 6 : 2	179.0 ± 22.4	0.25 ± 0.01	−29.97 ± 1.38	64.96 ± 0.32	2.82 ± 0.01
T3-2	20 : 2 : 6 : 3	193.2 ± 26.8	0.13 ± 0.01	−28.40 ± 0.91	41.80 ± 0.46	1.82 ± 0.01

[a] The SLCNs compositions are expressed as ratio of palmitic acid / cholesterol / TPGS / curcumin (w/w)

injected onto the HPLC system and the curcumin content was quantified at a wavelength of 425 nm. The data obtained were processed using the Chem Station software (Agilent technologies, Santa Clara, CA, USA). Calibration curves based on the ratios of areas of curcumin and resveratrol peaks to the curcumin concentration were found to be linear in the concentration range between 0.5 and 90 μg/mL. Linear regression analysis revealed that the equation of the line of best fit from the calibration graph was $y=0.1226\times-0.026$, with a good fit to the data ($r^2=0.99$).

Solid State Characterization

PXRD Analysis

The crystallographic structure of samples was characterized using powder X-ray diffractometer (PANalytical, Almelo, Netherlands) with a copper anode (Cu Kα radiation, 40 kV, 30 mA). Curcumin, palmitic acid, lyophilized plain SLN and SLCN samples were analyzed at ambient temperature, by scanning from 1° to 100, 2θ at 0.05° step size, and step time of 1.00 s.

DSC Analysis

The physical state and thermal behavior of the samples were characterized using a Mettler DSC apparatus (Mettler Toledo; Melbourne, Australia). For DSC measurements, 2 mg samples of each material (curcumin, palmitic acid, plain SLNs, and SLCNs) were loaded individually onto a standard aluminum pan and hermetically sealed. DSC analyses were performed under dry nitrogen gas with a flow rate of 50 mL/min, temperature range of 20–220°C, and scan rates of 10, 2.5, and 0.2°C/min.

TGA Analysis

The thermal decomposition of palmitic acid, curcumin, plain SLNs and CLSNs was measured using a thermogravimetric analyzer (Mettler Toledo, Greifensee, Switzerland). For each analysis, a 2 mg sample was weighed and placed in an aluminum pan. TGA analyses were performed under increasing temperature conditions (25°C to 500°C), with a heating rate of 10°C/min and under 20 mL/min nitrogen flow.

Compatibility Study- FT-IR Spectral Analysis

The potential interaction between the solid lipid core and incorporated drug was investigated using FT-IR studies (Bruker Analytik, Germany). The FT-IR analysis of pure curcumin, plain SLNs, and SLCNs were performed with a resolution of 2 cm^{-1} in the range between 4,000 and 500 cm^{-1}.

Preparation of TMC-SLCNs

The 20: 2: 6:1 w/w relative composition of palmitic acid, cholesterol, TPGS, and curcumin was found to be optimal, and was used for subsequent experiments. SLCNs were surface-modified with TMC by surface charge interaction. Solutions comprising equal volumes of negatively charged SLCNs and cationic TMC (50:1, w/w) were dispersed in distilled water and stirred for 10 h. Finally, TMC-SLCNs were collected by centrifugation at 13,000 rpm for 30 min and lyophilized. Similarly, CH-SLCNs were also prepared and used as control.

Stability Studies

Storage Stability Over 90 Days

The stability studies evaluating all lyophilized SLNs formulations were performed at different storage conditions and according to the modified ICH guidelines. The lyophilized samples were kept refrigerated temperature (2–8°C) and at room temperature. Immediately following synthesis and after 45 or 90 days of storage, particle size, zeta potential and EE were measured using the procedures described in the above sections.

Photostability

The photostability of lyophilized SLNs formulations were evaluated using the protocol described by C.S. Mangolim *et al* (29), with minor modification. The samples were placed into a petri dish and exposed to ambient sunlight and visible light for 0, 2 and 5 days. After exposure, specific quantity of each sample was withdrawn, and the quantity of curcumin was determined using HPLC-UV method.

In Vitro Release Studies

The cumulative release of curcumin from SLCNs and surface-modified SLCNs was measured using the dialysis bag diffusion technique as previously described (30,31), with minor modifications. SLN formulations containing 930 μg/mL curcumin were dispersed in simulated gastric fluid (SGF, pH 1.2) and simulated intestinal fluid (SIF, pH 7.4) solutions and transferred to a dialysis bag (molecular weight cutoff, 3 kDa). The dialysis bag was sealed at both ends and immersed in a receptor compartment containing the simulated medium. Samples were shaken horizontally in a shaker at 37±1°C and 50 strokes per minute. At predefined time intervals (0, 0.5, 1, 2, 3, 4, 6, 8, 12, and 24 h) a 1 mL sample of the medium was taken from the receptor compartment and replaced with the same volume of fresh medium to maintain sink conditions.

All collected samples were analyzed using HPLC-UV method.

In Vitro Cell Viability Studies

The antitumor efficacy of SLCNs formulations and non-toxic effect of plain SLNs was evaluated against human breast adenocarcinoma MCF-7 and mouse melanoma B16F10 cell lines by performing the MTT assay. Briefly, the cells were cultured in Dulbecco's Modified Eagle's Medium (DMEM), which was supplemented with 10% (v/v) fetal bovine serum (FBS), and 1% penicillin/ streptomycin, and kept at 37°C in a humidified 5% (v/v) CO_2 atmosphere in a sterile incubator. The cells were seeded 3×10^4 cells well in a 96 well plate and incubated at 37°C for 24 h. After incubation, 100 μL of the medium containing SLCN formulations at concentrations ranging from 1 to 20 μM were added to each well. After incubation for additional 24 or 48 h, the culture medium was replaced with 10 μL of 5 mg/mL MTT reagent and incubated at 37°C for 2 h. The medium was discarded and 100 μL of DMSO was added to each well. The plates were kept in the shaker to ensure the solubilization of formazan crystals in DMSO. Finally, the absorbance was measured at 570 nm by using a microplate reader (BioTek, Winooski, VT, USA). Relative cell viability was calculated from the absorbance of treated cells, by using non-treated cells as controls. All experiments were performed with $n=8$.

Pharmacokinetic Studies

Animals and Dosing

For *in vivo* pharmacokinetic studies, 4 week old male Balb/c mice weighing 20–25 g were used. All protocols involving experimental animal were approved by the Institutional Animal Ethics Committee of Gachon University, South Korea. The mice were randomly divided into four groups with $n=3$ in each group to minimize the variation between individuals. One group of animals received 50 mg/kg free curcumin diluted in 25% Tween 80 orally. The remaining groups received 50 mg/kg curcumin administered orally as SLN formulations comprising SLCNs, CH-SLCNs or TMC-SLCNs. All SLNs formulations were dispersed in distilled water just before oral administration. After administration, 20 μL of blood serial samples were withdrawn from the saphenous vein at 0.25, 0.5, 0.75, 1, 2, 4, and 8 h. Blood samples were collected in 0.5 mL of heparinized polythene tubes and centrifuged for 10 min at 4,000 rpm and, 4°C to obtain the plasma. Animals were sacrificed and decapitated at 8 h and the brains were carefully removed. All plasma samples and brain tissues were stored at −80°C until further LC-MS/MS analysis.

Quantification of Plasma and Brain Curcumin Content by LC-MS/MS

To quantify the amount of curcumin in the brain tissue, capillary depletion method was used (32). In brief, the brains were homogenized (ten strokes) in 0.8 mL of RHB-buffer using an ice-cold glass homogenizer. After addition of dextran (1.6 mL of 26% solution) another homogenization (three strokes) followed. The homogenate was separated into a supernatant (brain parenchymal fraction) and pellet (containing the vascular elements) by centrifugation for 15 min at 4°C and 5,400 g. Whole brain homogenate and separated brain fractions were analyzed for curcumin content after extraction.

Mouse plasma (10 μL) or brain homogenate samples (40 μL) were mixed with 10 μL of salbutamol internal standard (200 ng/mL) containing mobile phase and 10 μL of 0.5 M sodium hydroxide (to enhance the curcumin extraction) by vortexing for 1 min, prior to liquid-liquid extraction with 250 μL of ethyl acetate to isolate curcumin. After centrifugation for 10 min at 4°C and, 10,000 rpm, the organic layer was separated and evaporated to dryness under vacuum. Finally, the evaporated residue was reconstituted in 20 μL of mobile phase (acetonitrile and 0.01% formic acid, 50:50%, v/v) vortexed for 1 min, and used for LC-MS/MS analysis.

We developed and validated a highly sensitive, specific LC-MS/MS method for the quantitative analysis of curcumin in mouse plasma and brain tissue samples (manuscript submitted for publication). The Agilent HPLC (1100 series, Agilent Technologies) system connected to a 6490 triple quadrupole MS equipped with an ESI Agilent jet stream system was used for the LC-MS/MS measurement of curcumin levels in mouse plasma and brain homogenate samples. HPLC separation was conducted on an analytical Sepax BR-C18 (5 μm, 120 Å 1.0×100 mm) column, with the column temperature maintained at 30°C. The mobile phase consisted of acetonitrile and 0.1% formic acid (50: 50%, v/v) delivered at a constant flow of 0.2 mL/min. The injected volume of each sample was 2 μL. MS ionization was performed in the positive ESI mode with argon as a; collision gas, 5 kV; capillary voltage, 225°C gas temperature, 15.1 I/min gas flow, 40°C source temperature, and collision energies of 14 and 12 eV for curcumin and salbutamol, respectively. Analytes were quantified using multiple reactions monitoring (MRM) to monitor the ion transitions of 369–285 m/z for curcumin, and 240–148 m/z for salbutamol.

Kinetic Data and Statistical Analysis

The plasma concentration-time data were analyzed and the pharmacokinetic parameters, including maximum plasma concentration (C_{max}), corresponding time (T_{max}), area under the plasma concentration-time curve (AUC), elimination half-life ($t_{1/2}$), and mean residence time (MRT), were estimated

using non-compartmental analysis (NCA) in WinNonlin software (version 2.1, Pharsight, USA).

All data are presented as mean±S.D. Statistical significance was evaluated using ANOVA combined with Student's 't' tests, with analysis performed using Prism 4.0 software (Graph Pad software); *p*-values of 0.05 and below were considered significant.

RESULTS

Synthesis and Characterization of TMC Polymer

TMC with varying DQ values was synthesized and characterized as previously reported (14). Presence of *N*-trimethyl groups in the synthesized chitosan derivative was confirmed by ^{1}H-NMR and FT-IR spectral analyses. Characteristic peaks proving the presence of *N*-methylation were expected in the region of 2.47–3.37 ppm. A signal was detected at 3.25 ppm, which was attributed to the quaternized sites (Fig. 2b). TMC polymers with high DQ values 48% were obtained by amending the reaction step as described above.

The four characteristic bands in the FT-IR spectra of chitosan and TMC polymer correspond to the stretching vibration of NH_2 and OH combined peaks (3,425 cm^{-1}), C=O bonds of the acetamido groups (1,658 cm^{-1}), N-H bonds of the amino groups (1,564 cm^{-1}), and C-H bonds of methyl groups (1,479 cm^{-1}). The FT-IR spectra of chitosan and TMC were almost identical, with a distinguishing signal representing the deformation vibration of C-H at 1,479 cm^{-1} observed only the in TMC spectrum (Fig. 2c). FT-IR spectral analysis, therefore, indicated that the amino groups of chitosan were substituted by methyl groups.

Development and Optimization of SLCNs

Mean particle size, zeta potential, EE, and LC of optimized SLNs formulations are shown in Table I. The effect of palmitic acid concentration on particle size was determined by varying the concentration from 20 to 40 mg while keeping the same quantity of cholesterol (2 mg) and TPGS (6 mg). The results indicated that augmenting the palmitic acid concentration increased the particle size from 243.6±15.8 to 513.9±71.3 nm. Larger particle size may be caused by the higher viscosity of the dispersion medium at higher lipid concentrations, resulting in to larger particle size distributions (33,34). In addition, the surfactant is not able to completely cover the surface of the lipid core at high lipid concentrations, resulting in diminished emulsifying efficiency and supporting the particle agglomeration (35).

The curcumin EE was found to increase with increasing amounts of cholesterol without significantly affecting the mean particle size. The cholesterol at this concentration will provide additional space and sufficient rigidity to the nanoparticle which will be embedded between the phospholipid molecules. This will reduce the leakage of active therapeutic moiety from the nanocarriers. Additionally, presence of optimized proportion of cholesterol will act as a fluidizer or membrane rigidifying agent that will further increase the EE. In our study, EE increased in proportion to the mass of the lipid component, likely resulting from the hydrophobic interactions and high solubility of curcumin in palmitic acid and cholesterol.

The effect of relative amount of TPGS on particle size was evaluated by varying the TPGS concentration from 6 to 12 mg while maintaining the amount of palmitic acid (20 mg). High amounts of TPGS were found to result in an increase in the mean particle size. This might be attributed to the intrinsic thermodynamic instability of nanoparticles and hydrophobic interactions between TPGS molecules might be dominated, resulting in aggregation and increase in particle size. Our observations revealed that at very low concentrations, TPGS was adsorbed directly onto the surface of the particles. However, at high concentration of TPGS, creation of loops and tails and the compression of the emulsifier molecules at the surface of the solid lipid core were prominently observed and eventually led to the formation of bridges between the SLNs.

The effects of different concentrations of the curcumin loaded on the mean particle size and EE were evaluated using concentrations from 1 to 3 mg. The SLCNs system was stable up to 1 mg of curcumin with the solid lipid composition. However, our evaluation showed that the particle size significantly increased and EE decreased at curcumin concentrations above 1 mg. Each lipid evaluated was found to exhibit a distinct drug loading capacity, with the addition of excess amounts of drug leading to high levels of free, untrapped, drug in the formulation. Ultimately, the SLN composition comprising palmitic acid, cholesterol, TPGS, and curcumin at 20, 2, 6, and 1 mg, respectively, was found to be optimal for the formulation of small particles.

Surface Modification of SLCNs with TMC

Surface modification of the optimized SLCNs was performed using chitosan or TMC. Due to the high electrostatic interaction, chitosan or TMC were adsorbed onto the surface of SLCNs. Surface modification was evaluated by comparing the particle size and zeta potential of SLCNs before and after surface modification (Table II and Fig. 3). SLCNs with surface modification using chitosan or TMC presented with a greater particle size (mean diameter 311.9±67.7 nm, 412.0±79.7 nm), compared to that of the unmodified SLCNs (mean diameter 138.8±7.6 nm), clearly confirming that chitosan or TMC completely covered the surface of SLCNs. Furthermore, addition of chitosan or TMC reversed the

Table II Physicochemical Characterization of SLCNs (mean ± S.D, $n = 3$)

Group	Formulation	Particle size (nm)	PDI	Zeta potential (mV)	EE (%)	LC (%)
I	SLCNs	138.8 ± 7.6	0.15 ± 0.04	−29.67 ± 1.20	93.13 ± 0.11	4.04 ± 0.01
II	CH-SLCNs	311.9 ± 67.7[a]	0.24 ± 0.02	27.08 ± 0.86[a]	93.12 ± 0.06	4.04 ± 0.01
III	TMC-SLCNs	412.0 ± 79.7[a]	0.26 ± 0.09	35.70 ± 1.03[a]	93.12 ± 0.08	4.04 ± 0.01

[a] Significant difference with SLCNs ($p < 0.05$)

negative surface charge (zeta potential) of SLCNs from −29.67 ± 1.20 mV to 27.08 ± 0.86 mV, or 35.70 ± 1.03 mV, respectively, confirming that the SLCN surface was modified.

Evaluation of Particle EE

The EE of the SLCNs, CH-SLCNs and TMC-SLCNs was found to be 93.13 ± 0.11%, 93.12 ± 0.06% and 93.12 ± 0.08%, respectively. High lipophilicity of curcumin resulted in high EE of the drug in the solid lipid core, possibly due to the ability of palmitic acid and cholesterol to accommodate highly lipophilic molecules.

Physical State Characterization

PXRD Studies

Powder-XRD patterns obtained by analysis of pure curcumin, plain SLNs, SLCNs, and palmitic acid lipid matrix are presented in Fig. 4a. The powder-XRD diffractogram of pure curcumin exhibits numerous sharp peaks at 2 scattered angles, indicating its high crystallinity. By comparing the XRD patterns of SLCN and curcumin, SLCN patterns do not shown any crystalline peaks characteristic of curcumin, which indicates that curcumin was completely dispersed in the amorphous or molecular dispersion form within the crystal lattice of the lipid matrices. Additionally, there was no noticeable difference in diffraction patterns between plain SLNs and SLCNs indicating that the incorporation of curcumin into the SLNs did not affect the nature of SLNs. The diffraction patterns of SLCNs and lipid matrices were found to differ in intensity and resolution of the peaks, which primarily depend on factors such as particle size and quantity of sample (36). Amorphous form of curcumin has been used in SLNs to enhance the curcumin loading capacity, aqueous solubility, and oral bioavailability (37,38).

DSC Analysis

DSC is an important method for qualitative investigation of the physical states of free drug and drug encapsulated formulation by measuring the temperature and energy variation at the phase transition. DSC thermograms obtained by the analysis of curcumin, palmitic acid, plain SLNs, and SLCNs

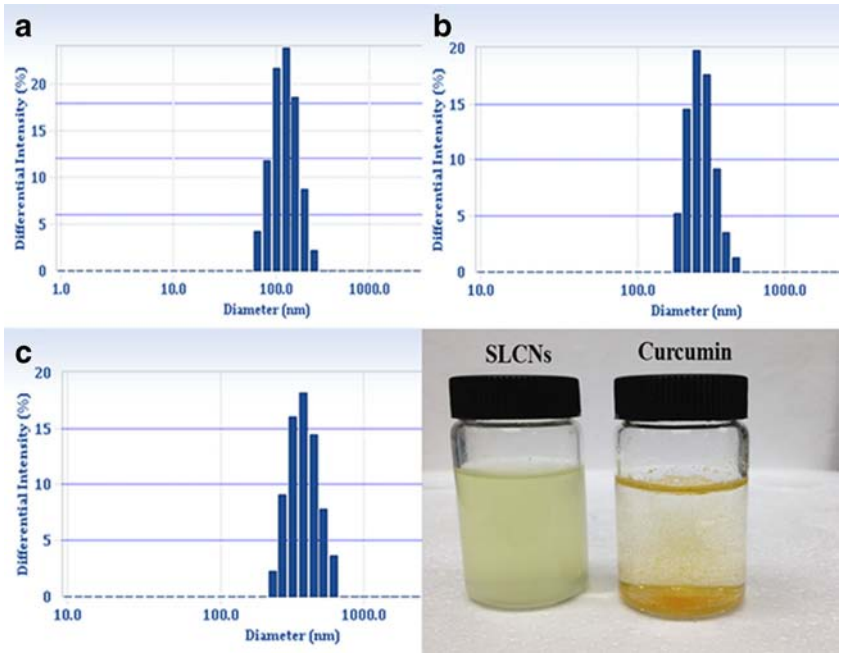

Fig. 3 Distribution of particle sizes of SLCNs (**a**), CH-SLCNs (**b**), TMC-SLCNs (**c**); comparative dispersibility of SLCNs and pure curcumin in distilled water (**d**).

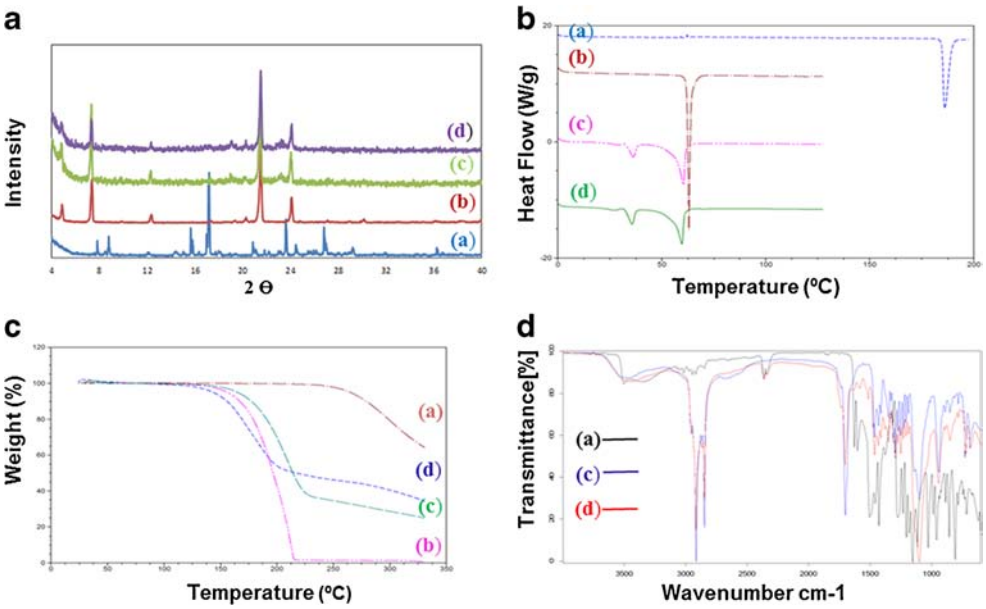

Fig. 4 Physical state of curcmin (**a**), (**b**) palmitic acid (**b**), (**c**) plain SLNs (**c**), and (**d**) SLCNs (**d**) evaluated by (**a**) P-XRD (**a**), (**b**) DSC (**b**), (**c**) TGA (**c**), and (**d**) FT-IR spectral analysis (**d**)

are shown in Fig. 4b. The curcumin thermogram showed a sharp endothermic peak at 183°C, corresponding to the melting point of curcumin and reflecting its crystalline nature. The palmitic acid thermogram had a peak at 63°C, which is related to the melting point of this lipid. The thermogram of SLCNs did not have any endothermic peaks at temperatures characteristic for curcumin, likely because of the higher degree of curcumin miscibility or entrapment within the solid lipid core. These findings are in agreement with the results of our entrapment efficiency analysis, which detected higher curcumin entrapment in the lipid core. The endothermic peak corresponding to the palmitic acid was slightly altered in SLCNs and plain SLNs because of the transformation of the lipid to a nanoparticle form and the presence of the drug, surfactant, and formulation additives.

TGA Studies

TGA analysis was used to determine the thermal stability of the free drug, lipids and drug embedded in the formulations. As shown in Fig. 4c, SLCNs formulation showed high thermal stability and negligible amount of mass loss at temperatures between 0 and 100°C. Therefore, curcumin and SLNs properties will not change during experiments at elevated temperature level.

FT-IR Spectral Analysis

The FT-IR spectra of pure drug, plain SLNs, and SLCNs are presented in Fig. 4d. FT-IR spectra of plain SLNs, SLCNs, and pure curcumin exhibit no peak shifting and no loss of characteristic functional group peaks. Therefore, our FT-IR analysis detected no interaction between curcumin and solid lipid core, suggesting that curcumin is compatible with the lipid component of SLNs as a drug formulation.

Stability Studies

Curcumin is recognized to be oxygen and photo sensitive, making the maintenance of its stability at different storage conditions a crucial parameter for its practical feasibility in potential clinical applications. The physical stability of lyophilized SLN formulations was determined by measuring the changes in particle size, zeta potential, and EE immediately after preparation, and after 45 or 90 days of storage under a range of conditions. No statistical difference was observed in measured parameters between the SLNs formulations kept refrigerated or at room temperature, ($p > 0.05$). After 0, 2 and 5 days of sun light and visible light exposure, the lyophilized SLN formulations exhibited that the curcumin remained stable from photodegradation and enhanced its stability (Fig. 5a, b and c). Based on these results showing excellent storage and photostability, SLN formulations stored at either refrigerated and room temperatures were used for subsequent studies and applications for active packaging.

In Vitro Release Studies

The *in vitro* release studies of curcumin from SLNs formulations were conducted in two different releases media: simulated gastric fluid (SGF, pH 1.2) and simulated intestinal fluid (SIF, pH 7.4). The cumulative release profile of curcumin is presented in Fig. 6a and b. Curcumin release was pH-dependent, with approximately 84.73 ± 1.34% and 67.35 ± 3.8% of

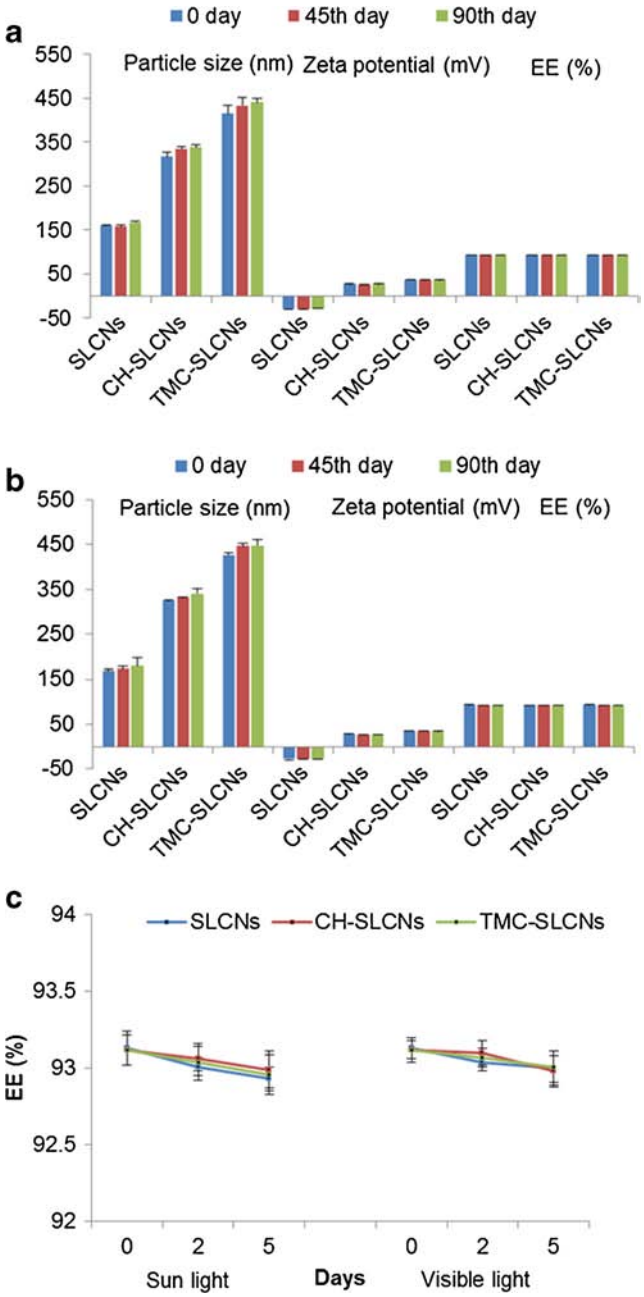

Fig. 5 Comparative stability studies of SLCNs, CH-SLCNs, and TMC-SLCNs evaluating particle size, zeta potential, and EE (%) following storage under refrigerated (**a**) and room temperature (**b**) conditions. Curcumin retention after 0, 2 and 5 days of exposure to sunlight and visible light (**c**). Data are presented as mean ± S.D ($n = 3$).

curcumin released from SLCNs in SGF and SIF after 24 h, respectively. The formulation of curcumin in CH-SLCNs resulted in release of 80.87 ± 1.90% and 48.19 ± 5.08% in SGF and SIF in 24 h, respectively. With both formulations the release rate of curcumin was higher in SGF than in SIF. Release of curcumin from TMC-SLCNs was negligible (8.71 ± 0.36%) in SGF and moderate (41.68 ± 2.39%) in SIF.

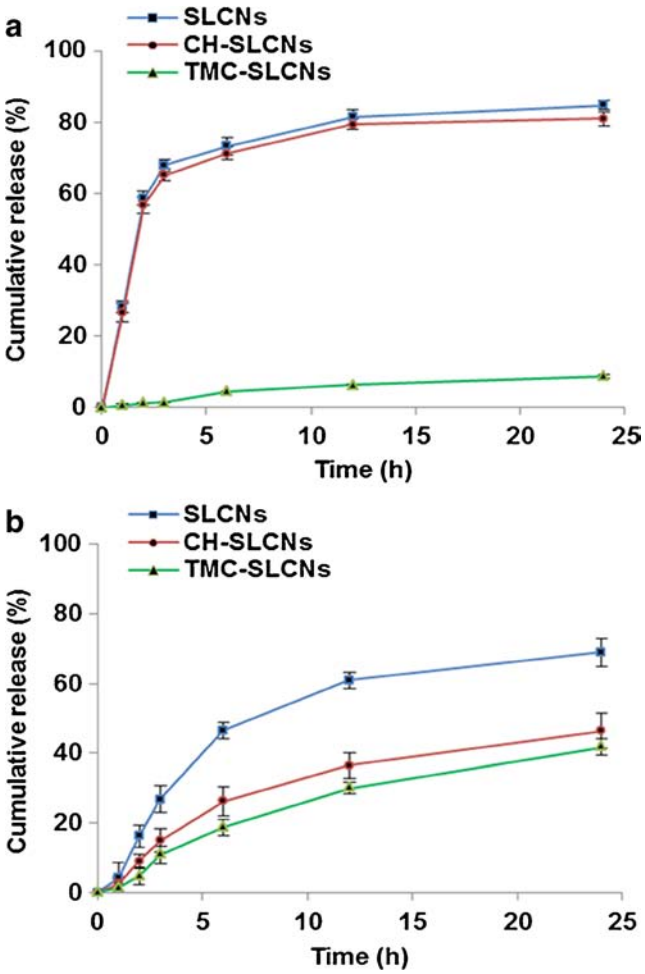

Fig. 6 Release profiles of curcumin from SLCNs, CH-SLCNs, and TMC-SLCNs in SGF (pH 1.2) (**a**) and SIF (pH 7.4) (**b**) evaluated up to 24 h. Statistically, significant difference was observed in the release of curcumin from SLCNs, CH-SLCNs, and TMC-SLCNs (***$p < 0.05$) Data represent means of cumulative percent curcumin release ± S.D ($n = 3$).

Cell Viability Studies

The *in vitro* effect of SLCNs on cell viability was investigated in MCF-7 and B16F10 cells by MTT assay. SLCNs were found to exhibit concentration and time-dependent cytotoxic effects on the cells. Cell viability (expressed as % of untreated cells) following incubation with different SLCNs formulations is presented in Fig. 7a and b. The treatment with plain SLNs was found to exert no cytotoxic effects on either of the studied cell lines. The inhibition of cell growth by SLCNs was enhanced when the incubation was prolonged from 24 to 48 h and SLCN concentration was increased 1 to 20 μM. SLCNs and surface-modified SLCNs showed a stronger *in vitro* antitumor effect compared to free curcumin. After 24 and 48 h of incubation, SLCNs and surface-modified SLNs elicited prolonged inhibitory effects on MCF-7 and B16F10 cells.

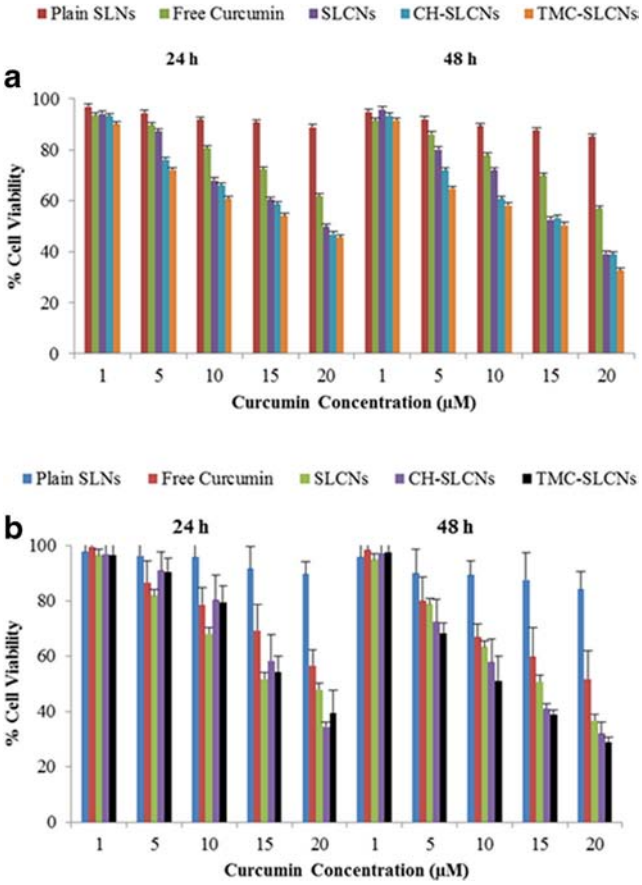

Fig. 7 *In vitro* cytotoxic effects of plain SLN, free curcumin, SLCNs, CH-SLCNs, and TMC-SLCNs in human breast adenocarcinoma MCF-7 (**a**), and mouse melanoma B16F10 (**b**) cell lines, evaluated by MTT assay following 24 or 48 h incubation.

Pharmacokinetic Studies

Improved Oral Bioavailability

To evaluate the pharmacokinetics of curcumin delivered using different vehicles, three SLN formulations (SLCNs, CH-SLCNs, and TMC-SLCNs) and a curcumin solution were orally administered to mice. Plasma concentration-time profiles of curcumin following oral administration of the formulations are presented in Fig. 8a, b and Table III. The curcumin suspension showed C_{max} of 0.24±0.05 μg/mL at 0.5 h (T_{max}) post administration, with the $AUC_{0\text{-}8h}$ value 0.27 ±0.03 h.μg/mL. These results clearly illustrate the characteristic drawbacks of the oral administration of curcumin, including poor oral absorption, enzymatic degradation, and rapid elimination. Conversely, curcumin administration in SLCNs and CH-SLCNs elicited significantly higher C_{max} values (0.58 ±0.03 and 0.69±0.16 μg/mL for SLCNs and CH-SLCNs, respectively), T_{max} of 2 h for both formulations and the $AUC_{0\text{-}8h}$ values of 1.85±0.36 and 2.08±0.49 h μg/mL for SLCNs and CH-SLCNs, respectively. Of all studied formulations, TMC-SLCNs displayed the optimal pharmacokinetic profile, with C_{max} of 1.21±0.12 μg/mL and $AUC_{0\text{-}8h}$ of 6.23± 0.75 h.μg/mL. T_{max} of all SLCNs formulations tested were found to be higher than the curcumin suspension. Significantly higher MRT compared to the curcumin suspension was observed, likely due to the sustained release of curcumin from SLNs. The $AUC_{0\text{-}\infty}$ measured following administration of all SLNs formulations were significantly higher than those observed following administration of the curcumin suspension suggesting that SLNs could protect curcumin from enzymatic degradation during the absorption process in the GI tract. TMC-SLCNs exhibited a longer $t_{1/2}$ (12.26±4.77 h) compared to the CH-SLCNs, C-SLNs, and curcumin solution confirming the prolonged drug residence following administration in TMC-SLCNs and longer absorption of curcumin in the GI tract.

Improved Curcumin Concentration in the Brain

The curcumin distributed in whole brain homogenate as well as in the pellet, and in the supernatant post oral administration was estimated at 8 h for curcumin suspension, SLCNs, CH-SLCNs and TMC-SLCNs. Figure 8c shows the curcumin distribution that were present in the brain fractions. Curcumin suspension, the curcumin concentration was not detectable in the homogenate. On the other hand, SLCNs, CH-SLCNs and TMC-SLCNs showed a detectable curcumin concentration in the homogenate, supernatant, and pellet after 8 h post administration. The results showed that curcumin from all the SLCNs formulations were chiefly distributed into the brain tissue than curcumin suspension. In comparison to other formulations, TMC-SLCNs showed higher curcumin concentrations in the homogenate and supernatant.

DISCUSSION

Considering the practical benefits of SLN formulations and the proven therapeutic efficacy of curcumin, the present study aimed to develop a novel drug delivery carrier system that would avoid the issues of decreasing the oral bioavailability of curcumin and prevent the burst release of carried drugs from the SLNs in acidic environments. In this study, SLN surface modification with chitosan and TMC were developed and investigated for enhancing the oral bioavailability of curcumin. Highly quaternized TMC was synthesized from chitosan by methylation. High DQ of methylated chitosan supports the use of this material to enhance absorption (39).

Our SLNs were formulated with palmitic acid and had a relatively small particle size (138.8±7.6 nm). Previous work has established that fatty acids with C-14 to C-18 carbon chains

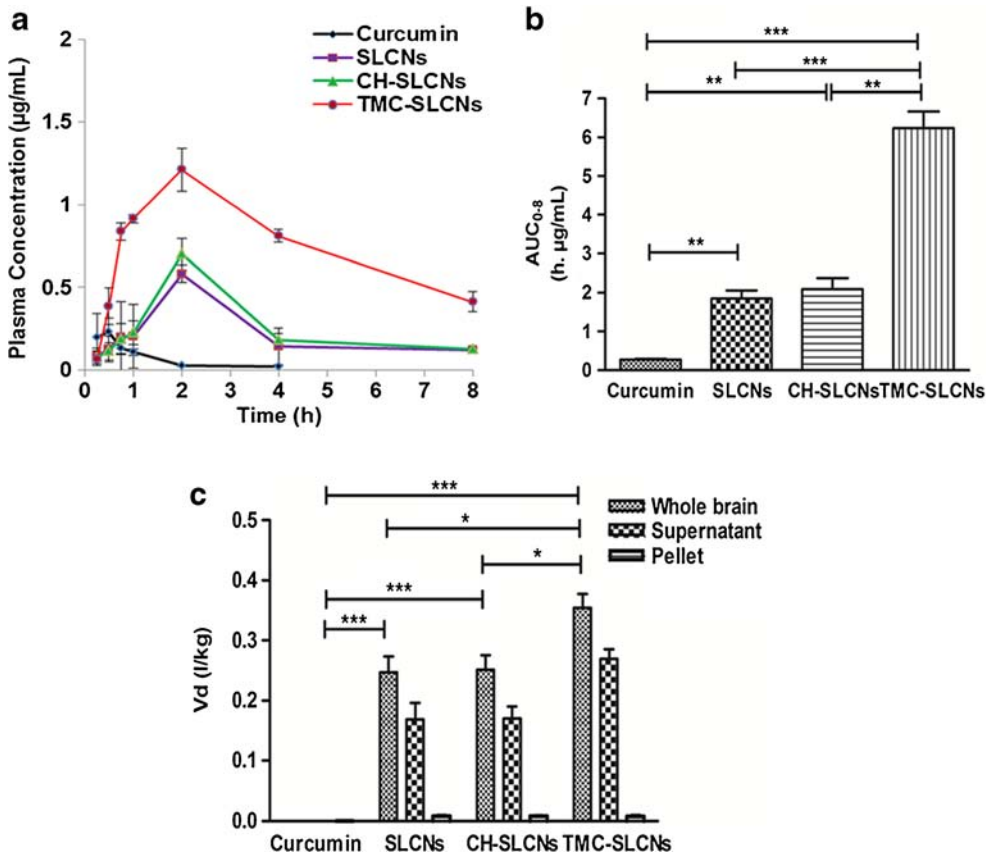

Fig. 8 (**a**) Plasma concentration-time profiles of curcumin in plasma and after oral administration of different curcumin formulations to mice at a dose of 50 mg/kg. (**b**) TMC-SLCNs showed higher plasma concentration and AUC to curcumin solution (***$p < 0.05$) and other SLCNs formulations (**$p < 0.05$). (**c**). Curcumin distribution in brain fractions were calculated using brain to plasma ratio of curcumin. The data suggest that the brain distribution significantly increased with TMC-SLCNs compared to curcumin suspension (***$p < 0.05$) and other SLCNs formulations (*$p < 0.05$). Data represents mean ± S.E ($n = 3$).

enhance intestinal absorption (40). From our studies, both the entrapment efficiency and the drug loading capacity were enhanced when cholesterol was included in the SLNs formulations. Cholesterol decreases the lipid fluidity and delays the drug leakage from the SLNs. The choice of emulsifier is another crucial parameter determining the stability of the SLNs formulations. Despite its common use as an emulsifier, poly(vinyl alcohol) (PVA) may be toxic when used in nanoformulations due to the formation of an interconnected network at the interface with nanoparticles, which makes PVA difficult to remove after emulsification (41). Hydrophilic–lipophilic balance value in the 12–16 range is considered optimal for the preparation of a stable *O/W* emulsion. In Comparison with PVA, TPGS is an effective, safe alternative emulsifier with HLB value (13.2) in the favorable range. Residual TPGS on the surface of nanoparticles can be easily and completely removed by washing, which permits the nanoparticles to be utilized for subsequent surface modifications (41). Among several methods available for the preparation of SLNs, combination of high shear homogenization and ultrasonication is a rapid and straightforward technique that effectively formulates monodispersed SLNs. Following optimization of SLCNs composition, particles were characterized for size, PDI, zeta potential, entrapment efficiency, loading capacity, crystallinity, thermal stability

Table III Pharmacokinetic parameters of curcumin after oral admisistration of curcumin solution, SLCNs, CH-SLCNs and TMC-SLCNs (mean ± S.D, $n = 3$)

Formulation	T_{max} (h)	C_{max} (µg/ml)	$AUC_{0\text{-}8h}$ (h. µg/ml)	$AUC_{0\text{-}\infty}$ (h. µg/ml)	AUMC	MRT (h)	$t_{1/2}$(h)	Relative F (%)
Curcumin	0.5	0.24 ± 0.02	0.27 ± 0.02	0.31 ± 0.02	0.30 ± 0.01	1.13 ± 0.07	1.11 ± 0.19	1
SLCNs	2	0.58 ± 0.02[a]	1.85 ± 0.21[a]	6.01 ± 1.11[a]	5.84 ± 0.65[a]	3.16 ± 0.01[a]	5.79 ± 0.68[a]	6.85
CH-SLCNs	2	0.69 ± 0.09[a]	2.08 ± 0.28[a]	6.94 ± 2.24[a]	6.53 ± 0.76[a]	3.15 ± 0.12[a]	5.19 ± 0.86[a]	7.70
TMC-SLCNs	2	1.21 ± 0.13[a,b]	6.23 ± 0.43[a,b]	12.76 ± 0.01[a,b]	22.87 ± 1.71[a,b]	3.67 ± 0.03[a]	12.26 ± 2.75[a,b]	23.07

T_{max}: Time to maximum plasma concentration; C_{max}: Maximum concentration; $AUC_{(0\text{-}8h)}$: Area under the curve up to the 8 h; $AUC_{(0\text{-}\infty)}$: AUC up to infinite time; AUMC: Area under the moment curve; MRT: Mean residence time; $t_{1/2}$: terminal phase half-life

Relative F values are calculated as a ratio of AUC of the formulation to that of the curcumin

[a] Statictical significance with curcumin, $p < 0.05$

[b] Statictical signifance with SLCNs, $p < 0.05$

and compatibility. The 20:2:6:1 relative composition of palmitic acid, cholesterol, TPGS, and curcumin was identified as optimal for the preparation of both CH-SLCNs and TMC-SLCNs.

Evaluation of particle sizes and zeta potentials confirmed the surface modification on SLCNs. Our TMC-SLCNs exhibited a relatively high positive zeta potential value (35.70± 1.03 mV) allowing long-term contact of SLNs with the epithelium linings, as well as colloidal stability. No significant differences in EE and LC of CH-SLCNs and TMC-SLCNs were observed upon surface modification. This implies that during the surface modification process, no drug was released from the intact core. Furthermore, during the polyelectrolyte assembly process, drug was retained either within the core or within the polymer mesh on the surface. This is in addition to the fact that large cavity size of our particles could accommodate larger quantities of drugs. All SLN formulations were found to be stable when stored refrigerated, as well as at room temperature. Furthermore, the oxygen and photosensitivity of curcumin were significantly decreased by entrapping curcumin into our SLN carrier system. The *in vitro* release of curcumin from the SLNs formulations was evaluated in simulated GI conditions. The cumulative release of curcumin from both SLCNs and CH-SCLNs was significantly higher in acidic conditions compared to the basic medium, probably because of the swelling of chitosan, protonation under acidic condition, and the previously demonstrated burst release of SLNs. Even though SLCNs and CH-SLCNs showed sustained release in SIF, the burst release of curcumin in SGF precludes the use of these formulations in oral drug delivery systems. The surface modification of SLCNs with TMC has been proposed as an approach to avoid burst release of carried drugs. The excellent stability resulting from the TMC-mediated protection of SLNs in acidic conditions effectively prevents burst release of drugs in the gastric environment. Since TMC, unlike chitosan, is a water soluble polymer that remains soluble under intestinal pH conditions, TMC SLCNs can be useful for controlled oral delivery of curcumin.

Finally, we performed *in vivo* evaluations of the surface-modified and other SLCN formulations to assess their potential for improving oral bioavailability and brain distribution of curcumin in mice. TMC-SLCNs showed higher relative bioavailability of curcumin (23.07%) in comparison to the curcumin solution (1%). Compared to SLCNs and CH-SLCNs, TMC-SLCNs were found to successfully protect the SLNs from hostile GI environment. Surface modification with TMC may therefore protect SLNs in the stomach, resulting in a sustained release of curcumin in the intestinal tract and higher curcumin levels in the blood circulation. Hence, TMC coated SLCNs and other SLCNs formulations improved the curcumin concentration in brain as compare to curcumin suspension. Thus, the results of the present study proved that a large quantity of curcumin crossed the BBB after oral administration and higher accumulation in the brain parenchymal compartment than vascular pellet, thereby improving its bioavailability. Higher plasma concentration and brain distribution of oral curcumin administered as a TMC-SLCN formulation could be a result of a number of factors. Positively charged TMC have high affinity with negative sites present on cell membranes because of ionic interaction. Additionally, TMC-SLCNs may enhance the permeation of curcumin through a paracellular transport mechanism by opening the tight junction between epithelial cells and sustained delivery of drug to the brain. Overall, the results of our study suggest that TMC surface-modified SLNs might be a promising nanocarrier system that can be used to improve the oral bioavailability and brain distribution of curcumin.

CONCLUSIONS

We successfully prepared and characterized a trimethyl derivative of chitosan and developed a novel nanocarrier system of SLN surface-modified with TMC, with potential application for the oral delivery and brain distribution of curcumin. The excellent stability resulting from the TMC-mediated protection of SLNs in acidic conditions effectively prevents burst release of drugs in the gastric environment. In summary, this study showed that TMC-SLNCs can be used as carrier particles to improve the oral bioavailability and brain distribution of the curcumin. Further investigation of TMC-SLCNs in the treatment of Alzheimer's disease and brain gliomas by using animal models will be performed to obtain *in vivo* data supporting future clinical applications.

ACKNOWLEDGMENTS

This research was supported by the Basic Science Research Program of Korean National Research Foundation (NRF-20110007794).

REFERENCES

1. Maheshwari RK, Singh AK, Gaddipati J, Srimal RC. Multiple biological activities of curcumin: a short review. Life Sci. 2006;78(18):2081–7.
2. Tang H, Murphy CJ, Zhang B, Shen Y, Van Kirk EA, Murdoch WJ, *et al.* Curcumin polymers as anticancer conjugates. Biomaterials. 2010;31(27):7139–49.
3. Mondal G, Barui S, Saha S, Chaudhuri A. Tumor growth inhibition through targeting liposomally bound curcumin to tumor vasculature. J Control Release. 2013;172(3):832–40.
4. Sun J, Bi C, Chan HM, Sun S, Zhang Q, Zheng Y. Curcumin-loaded solid lipid nanoparticles have prolonged in vitro antitumour activity, cellular uptake and improved in vivo bioavailability. Colloids Surf B: Biointerfaces. 2013;111:367–75.

5. Mehnert W, Mäder K. Solid lipid nanoparticles: production, characterization and applications. Adv Drug Deliv Rev. 2012;64:83–101.
6. Müller RH, Mäder K, Gohla S. Solid lipid nanoparticles (SLN) for controlled drug delivery—a review of the state of the art. Eur J Pharm Biopharm. 2000;50(1):161–77.
7. Venkateswarlu V, Manjunath K. Preparation, characterization and in vitro release kinetics of clozapine solid lipid nanoparticles. J Control Release. 2004;95(3):627–38.
8. Venishetty VK, Chede R, Komuravelli R, Adepu L, Sistla R, Diwan PV. Design and evaluation of polymer coated carvedilol loaded solid lipid nanoparticles to improve the oral bioavailability: a novel strategy to avoid intraduodenal administration. Colloids Surf B: Biointerfaces. 2012;95:1–9.
9. Madan J, Pandey RS, Jain V, Katare OP, Chandra R, Katyal A. Poly (ethylene)-glycol conjugated solid lipid nanoparticles of noscapine improve biological half-life, brain delivery and efficacy in glioblastoma cells. Nanomedicine Nanotechnol Biol Med. 2013;9(4):492–503.
10. Agnihotri SA, Mallikarjuna NN, Aminabhavi TM. Recent advances on chitosan-based micro- and nanoparticles in drug delivery. J Control Release. 2004;100(1):5–28.
11. Amidi M, Romeijn SG, Borchard G, Junginger HE, Hennink WE, Jiskoot W. Preparation and characterization of protein-loaded N-trimethyl chitosan nanoparticles as nasal delivery system. J Control Release. 2006;111(1–2):107–16.
12. Thanou M, Verhoef JC, Junginger HE. Oral drug absorption enhancement by chitosan and its derivatives. Adv Drug Deliv Rev. 2001;52(2):117–26.
13. Chen F, Zhang Z-R, Yuan F, Qin X, Wang M, Huang Y. In vitro and in vivo study of N-trimethyl chitosan nanoparticles for oral protein delivery. Int J Pharm. 2008;349(1–2):226–33.
14. Subbiah R, Ramalingam P, Ramasundaram S, Kim DY, Park K, Ramasamy MK, *et al.* N, N, N-Trimethyl chitosan nanoparticles for controlled intranasal delivery of HBV surface antigen. Carbohydr Polym. 2012;89(4):1289–97.
15. Jintapattanakit A, Junyaprasert VB, Mao S, Sitterberg J, Bakowsky U, Kissel T. Peroral delivery of insulin using chitosan derivatives: a comparative study of polyelectrolyte nanocomplexes and nanoparticles. Int J Pharm. 2007;342(1):240–9.
16. Sandri G, Rossi S, Bonferoni MC, Ferrari F, Zambito Y, Colo GD, *et al.* Buccal penetration enhancement properties of N -trimethyl chitosan: influence of quaternization degree on absorption of a high molecular weight molecule. Int J Pharm. 2005;297(1):146–55.
17. Di Colo G, Burgalassi S, Zambito Y, Monti D, Chetoni P. Effects of different N-trimethyl chitosans on in vitro/in vivo ofloxacin transcorneal permeation. J Pharm Sci. 2004;93(11):2851–62.
18. Florea BI, Thanou M, Junginger HE, Borchard G. Enhancement of bronchial octreotide absorption by chitosan and N -trimethyl chitosan shows linear in vitro/in vivo correlation. J Control Release. 2006;110(2):353–61.
19. He W, Du Y, Dai W, Wu Y, Zhang M. Effects of N-trimethyl chitosan chloride as an absorption enhancer on properties of insulin liquid suppository in vitro and in vivo. J Appl Polym Sci. 2006;99(3):1140–6.
20. Sayın B, Somavarapu S, Li XW, Sesardic D, Şenel S, Alpar OH. TMC–MCC (N-trimethyl chitosan–mono-N-carboxymethyl chitosan) nanocomplexes for mucosal delivery of vaccines. Eur J Pharm Sci. 2009;38(4):362–9.
21. Yin L, Ding J, He C, Cui L, Tang C, Yin C. Drug permeability and mucoadhesion properties of thiolated trimethyl chitosan nanoparticles in oral insulin delivery. Biomaterials. 2009;30(29):5691–700.
22. Cafaggi S, Russo E, Stefani R, Leardi R, Caviglioli G, Parodi B, *et al.* Preparation and evaluation of nanoparticles made of chitosan or N -trimethyl chitosan and a cisplatin–alginate complex. J Control Release. 2007;121(1):110–23.
23. Germershaus O, Mao S, Sitterberg J, Bakowsky U, Kissel T. Gene delivery using chitosan, trimethyl chitosan or polyethylenglycol-graft-trimethyl chitosan block copolymers: establishment of structure–activity relationships in vitro. J Control Release. 2008;125(2):145–54.
24. Chen H, Wu J, Sun M, Guo C, Yu A, Cao F, *et al.* N-trimethyl chitosan chloride-coated liposomes for the oral delivery of curcumin. J Liposome Res. 2012;22(2):100–9.
25. Slütter B, Soema PC, Ding Z, Verheul R, Hennink W, Jiskoot W. Conjugation of ovalbumin to trimethyl chitosan improves immunogenicity of the antigen. J Control Release. 2010;143(2):207–14.
26. Zhang Z, Tan S, Feng S-S. Vitamin E TPGS as a molecular biomaterial for drug delivery. Biomaterials. 2012;33(19):4889–906.
27. Ramasamy TG, Haidar ZS. Formulation, characterization and cytocompatibility evaluation of novel coreshell solid lipid nanoparticles for the controlled and tunable delivery of a model protein. J Bionanoscience. 2011;5(2):143–54.
28. Zanotto-Filho A, Coradini K, Braganhol E, Schröder R, de Oliveira CM, Simões-Pires A, *et al.* Curcumin-loaded lipid-core nanocapsules as a strategy to improve pharmacological efficacy of curcumin in glioma treatment. Eur J Pharm Biopharm. 2013;83(2):156–67.
29. Mangolim CS, Moriwaki C, Nogueira AC, Sato F, Baesso ML, Neto AM, *et al.* Curcumin–β-cyclodextrin inclusion complex: Stability, solubility, characterisation by FT-IR, FT-Raman, X-ray diffraction and photoacoustic spectroscopy, and food application. Food Chem. 2014;153:361–70.
30. Zhang J, Tang Q, Xu X, Li N. Development and evaluation of a novel phytosome-loaded chitosan microsphere system for curcumin delivery. Int J Pharm. 2013;448(1):168–74.
31. Kakkar V, Singh S, Singla D, Kaur IP. Exploring solid lipid nanoparticles to enhance the oral bioavailability of curcumin. Mol Nutr Food Res. 2011;55(3):495–503.
32. Wohlfart S, Khalansky AS, Gelperina S, Begley D, Kreuter J. Kinetics of transport of doxorubicin bound to nanoparticles across the blood–brain barrier. J Control Release. 2011;154(1):103–7.
33. Mehnert W, Mäder K. Solid lipid nanoparticles: production, characterization and applications. Adv Drug Deliv Rev. 2001;47(2–3):165–96.
34. Chen C-C, Tsai T-H, Huang Z-R, Fang J-Y. Effects of lipophilic emulsifiers on the oral administration of lovastatin from nanostructured lipid carriers: physicochemical characterization and pharmacokinetics. Eur J Pharm Biopharm. 2010;74(3):474–82.
35. Subedi RK, Kang KW, Choi H-K. Preparation and characterization of solid lipid nanoparticles loaded with doxorubicin. Eur J Pharm Sci. 2009;37(3–4):508–13.
36. de Carvalho SM, Noronha CM, Floriani CL, Lino RC, Rocha G, Bellettini IC, *et al.* Optimization of α-tocopherol loaded solid lipid nanoparticles by central composite design. Ind Crop Prod. 2013;49:278–85.
37. Pawar YB, Shete G, Popat D, Bansal AK. Phase behavior and oral bioavailability of amorphous Curcumin. Eur J Pharm Sci. 2012;47(1):56–64.
38. Mulik RS, Mönkkönen J, Juvonen RO, Mahadik KR, Paradkar AR. Transferrin mediated solid lipid nanoparticles containing curcumin: enhanced in vitro anticancer activity by induction of apoptosis. Int J Pharm. 2010;398(1–2):190–203.
39. van der Merwe SM, Verhoef JC, Verheijden JHM, Kotzé AF, Junginger HE. Trimethylated chitosan as polymeric absorption enhancer for improved peroral delivery of peptide drugs. Eur J Pharm Biopharm. 2004;58(2):225–35.
40. Porter CJH, Charman WN. Intestinal lymphatic drug transport: an update. Adv Drug Deliv Rev. 2001;50(1–2):61–80.
41. Wang ZH, Wang ZY, Sun CS, Wang CY, Jiang TY, Wang SL. Trimethylated chitosan-conjugated PLGA nanoparticles for the delivery of drugs to the brain. Biomaterials. 2010;31(5):908–15.